


Detection of Crossed Cerebellar Diaschisis by Intravoxel Incoherent Motion MR Imaging in Subacute Ischemic Stroke

Cell Transplantation
2019, Vol. 28(8) 1062–1070
© The Author(s) 2019
Article reuse guidelines:
sagepub.com/journals-permissions
DOI: 10.1177/0963689719856290
journals.sagepub.com/home/cit


Juan Wang^{1,2} , Shiteng Suo¹, Jinyan Zu^{1,2}, Wanqiu Zhu¹, Lijun Pan¹, Shaoli Song³, Yang Li², Lei Li², Zengai Chen^{1,2}, and Jianrong Xu¹

Abstract

Intravoxel incoherent motion has received extensive attention in brain studies for its potential as a non-invasive magnetic resonance perfusion method. However, studies on intravoxel incoherent motion imaging and crossed cerebellar diaschisis detection are relatively scarce. The aim of our study was to evaluate the feasibility of using intravoxel incoherent motion imaging in crossed cerebellar diaschisis diagnosis in subacute ischemic stroke patients by comparing results from intravoxel incoherent motion imaging, single-photon emission computed tomography, and arterial spin-labeling perfusion methods. In total, 39 patients with subacute ischemic stroke who underwent intravoxel incoherent motion, arterial spin-labeling, and single-photon emission computed tomography scanning were enrolled. Intravoxel incoherent motion-derived perfusion-related parameters including fast diffusion coefficient, vascular volume fraction, arterial spin-labeling-derived cerebral blood flow as well as single-photon emission computed tomography-derived cerebral blood flow of bilateral cerebellum were measured. A crossed cerebellar diaschisis-positive result was considered present with an asymmetry index $\geq 10\%$ of single-photon emission computed tomography. In the crossed cerebellar diaschisis-positive group, fast diffusion coefficient, arterial spin-labeling-derived cerebral blood flow, and computed tomography-derived cerebral blood flow of the contralateral cerebellum decreased compared with those of the ipsilesional cerebellum; whereas vascular volume fraction significantly increased. The National Institutes of Health Stroke Scale score and infarct volume in the crossed cerebellar diaschisis-positive group were significantly higher than those in the crossed cerebellar diaschisis-negative group. A positive correlation was detected between the fast diffusion coefficient-based asymmetry index and the single-photon emission computed tomography-based asymmetry index, fast diffusion coefficient-based asymmetry, and arterial spin-labeling based asymmetry index; whereas the vascular volume fraction-based asymmetry index value had a negative correlation with the single-photon emission computed tomography-based asymmetry index and arterial spin-labeling based asymmetry index. Furthermore, the area under the receiver operating characteristic curve value of the arterial spin-labeling-based asymmetry index was 0.923. The fast diffusion coefficient derived from the intravoxel incoherent motion could be valuable for the assessment of crossed cerebellar diaschisis in supratentorial stroke patients.

Keywords

Intravoxel incoherent motion, crossed cerebellar diaschisis, arterial spin-labeling, stroke

Introduction

When an ischemic cerebral stroke occurs, a series of excitotoxicity, apoptosis, and cell death is activated, which may lead to morbidity and mortality¹. As a common radiological phenomenon, crossed cerebellar diaschisis (CCD) is characterized by hypoperfusion and hypometabolism of the contralateral cerebellar hemisphere, which results from the dysfunction of the related supratentorial region². CCD has been reported in many acute and chronic brain diseases, such as supratentorial stroke, cerebral hemorrhage, infection,

¹ Department of Radiology, Renji Hospital, China

² Department of Radiology, Renji Hospital South Campus, China

³ Department of Nuclear Medicine, Renji Hospital South Campus, China

Submitted: July 28, 2018. Revised: April 23, 2019. Accepted: May 8, 2019.

Corresponding Authors:

Zengai Chen, Department of Radiology, Renji Hospital, School of Medicine, Shanghai Jiao Tong University, Shanghai, China.

Email: chenzengai@163.com

Jianrong Xu, Department of Radiology, Renji Hospital South Campus, School of Medicine, Shanghai Jiao Tong University, Shanghai, China.

Email: xujianrong_renji@163.com



tumor, and epilepsy³⁻⁷. Growing evidence indicates that CCD plays an important role in assessing neurological improvement and clinical outcomes after infarction⁸⁻¹⁰. For example, Takasawa et al. have shown that the severity of asymmetry indices (AI) of single-photon emission computed tomography (SPECT) in the early subacute stage correlates significantly with both the final modified Rankin scale and the Barthel Index scores, two indices that represented the clinical outcome⁹. These findings imply that CCD may be a valuable predictor of functional impairment in patients suffering supratentorial infarction.

CCD manifests as decreased cerebellar cerebral blood flow (CBF), which was first observed in a stroke patient using positron emission tomography (PET) in 1981¹¹. Based on our knowledge, PET and SPECT have been established as the reference standards for CCD detecting^{12,13}. However, the two methods involve the contrast agent injection and radiation exposure, which would inevitably limit their clinical use due to critical concerns among patients. With the development of magnetic resonance (MR) perfusion techniques, many researchers have tried to assess CCD through radiation-free methods. For instance, dynamic susceptibility contrast perfusion-weighted imaging was found to be able to identify CCD by various parameters but the detection rate was lower than PET/SPECT¹². Chen et al. also observed that arterial spin-labeling (ASL) was useful to detect CCD after stroke because of the consistent results with PET/SPECT series¹⁴.

Intravoxel incoherent motion (IVIM) MR imaging (MRI), a method that measures the relationship between signal attenuation with multiple b values, could simultaneously estimate the diffusion and perfusion parameters in a noninvasive way¹⁵. Le Bihan et al. initially obtained the images of diffusion and perfusion through IVIM imaging technique in brain tumor and ischemia¹⁶. By applying the bi-exponential model, several parameters such as the slow diffusion coefficient (D), the pseudodiffusion fast diffusion coefficient (D^*), and the perfusion vascular volume fraction (f) could be obtained from IVIM^{17,18}. With the development of IVIM, many researchers have explored and revealed the diagnostic value of IVIM in various diseases^{18,19}, including ischemic stroke¹⁵. In the previously mentioned IVIM study on stroke, decreases in D , D^* , and f were found in the ischemic stroke hemisphere compared with the contralateral side, which was in accordance with the pathophysiology of stroke²⁰. Another IVIM study also showed a reduction in f in the infarcted area in acute stroke²¹. According to our literature review, limited information exists on whether IVIM could detect CCD phenomenon in brain diseases.

Thus, the aim of this study was to evaluate the feasibility of using IVIM MRI in CCD diagnosis in patients with subacute supratentorial stroke and compare the results from IVIM with those from SPECT and ASL in identifying CCD.

Materials and Methods

Patients

The whole study followed approval from the hospital institutional research ethics board, and all subjects have written informed consent. A retrospective review of our institution's clinical and imaging database identified 56 patients who were diagnosed with subacute ischemic stroke from August 2013 to December 2014 and underwent IVIM and ASL MRI and SPECT. The definition of subacute stroke was 24 h to approximately 2 weeks from onset according to the study by Kim et al²².

Among these patients, 17 were excluded for having one or more of the following conditions: (1) infarct in the brain stem, cerebellum, or bilateral supratentorial infarct; (2) history of intracranial tumor, head trauma, subarachnoid hemorrhage, arteriovenous malformation, or brain surgery; (3) abnormalities in the posterior fossa on T₁, T₂, and diffusion-weighted MR images; (4) MR angiography showing angiopathy of vertebral basilar artery and the major branches. Of the 39 study patients, 25 were men (mean age 60.6 years; age range 34.0–84.0 years) and 14 were women (mean age 65.64 years; age range 43.0–84.0 years), with an overall mean age of 62.41 years (age range 34.0–84.0 years). The mean duration from stroke onset to MRI in the CCD-positive and the CCD-negative groups were 6.52 ± 3.54 days and 5 ± 3 days, respectively. Meanwhile, the mean time interval from stroke onset to SPECT was 5.75 ± 2.94 days and 4.9 ± 4.84 days, respectively. The National Institutes of Health Stroke Scale (NIHSS) was used to evaluate the neurological and functional status at the time of the admission and at discharge (14 days later).

MRI

All MRI examinations were performed on a 3-T platform (HDxt; General Electric Medical Systems, Waukesha, WI, USA) with a standard eight-channel phased array head coil. The imaging protocol included T1-weighted, T2-weighted, MR angiography, ASL, and IVIM imaging sequences. IVIM imaging was performed through multi b -value diffusion-weighted imaging using a single-shot spin-echo echo planar imaging sequence with the diffusion-weighted gradients along three orthogonal directions and the following parameters: repetition time/echo time = 6000/88 ms, field of view = 260×260 mm², matrix size = 192×192 , in-plane resolution = 1.35×1.35 mm², 18 slices with a slice thickness/spacing of 5/1.5 mm, bandwidth = 1950 Hz, acceleration factor = 2, number of averages = 2, b values = 0, 20, 50, 100, 150, 200, 500, 800, and 1000 s/mm², and acquisition time = 5 min. Pseudo-continuous ASL perfusion images were collected using three-dimensional (3D) fast spin echo acquisition with background suppression, with a post labeling delay of 1500 ms. Other parameters were repetition time/echo time = 4601/10.5 ms, field of view = 240×240 mm², matrix size = 128×128 , 38 slices with a slice thickness of 4 mm, and number of averages = 3.

Table 1. Comparison of characteristics between CCD (+) and CCD (-) subjects.

Characteristics	All (n=39)	CCD+ (n=13)	CCD- (n=26)	p value
Age (year)	62.41 ± 12.97	62.46 ± 14.65	62.38 ± 12.36	0.731
Gender, male/female	25/14	7/6	18/8	0.482
Infarct volume (mm ³)	11873 ± 22993	28208 ± 33981	3705 ± 6418	0.042*
Admission NIHSS	3.15 ± 2.21	4.46 ± 2.57	2.5 ± 1.72	0.02*
Discharge NIHSS	2.64 ± 2.19	4.00 ± 2.45 ^a	1.96 ± 1.73 ^b	0.011*
Location				
Gray matter	12 (30.8%)	8 (61.5%)	4 (15.4%)	0.005*
White matter	23 (59%)	5 (38.4%)	18 (69.2%)	0.09
Thalamus	4 (10.26%)	0 (0%)	4 (15.38%)	0.182

CCD: crossed cerebellar diaschisis; NIHSS: National Institutes of Health Stroke Scale.

Values are mean ± standard deviation or number of patients.

*Results indicated a significant difference ($p < 0.05$), p values refer to the Mann-Whitney U test, Fisher's exact test as appropriate.

^aNot significantly different ($p = 0.724$) between admission and discharge NIHSS score in the CCD (+) group.

^bSignificantly different ($p = 0.021$) between admission and discharge NIHSS score in the CCD (-) group.

SPECT imaging

SPECT was performed in all patients in a silent, dimly lit room with their eyes open and ears unplugged. Approximately 20–25 minutes after intravenous injection of 925–1110 MBq (25–30 mCi) technetium-99methylcysteinatedimer (HAT Co. Ltd. Shanghai, China), data acquisition was done on a dual-headed rotating scintillation gamma camera (Infinia Hawkeye 4, General Electric Medical Systems) with the patient supine, headrest attached, smallest permissible radius of rotation, 128 × 128 matrix, 360°, 120 projections, 25 seconds per view for a total 64 views by using a low-energy high-resolution parallel hole collimator. A 20% window centered at a 140 KeV photopeak for Tc-^{99m} was used. Raw data were smoothed with the Butterworth filter.

Imaging data processing

IVIM-MRI images were transferred to the dedicated workstation (ADW 4.5; General Electric Medical Systems) for post-processing. IVIM parameters including D , D^* , and f were calculated by using the bi-exponential model expressed as follows:

$$\frac{S(b)}{S_0} = fe^{-bD^*} + (1-f)e^{-bD}$$

where $S(b)$ and S_0 denote the signal intensity at the b values of b and 0, respectively, D and D^* are the diffusion coefficient related to molecular diffusion and the pseudodiffusion coefficient related to microcapillary perfusion, respectively, and f is the perfusion fraction.

The standard apparent diffusion coefficient (ADC) was calculated using the conventional mono-exponential model with all b values:

$$\frac{S(b)}{S_0} = e^{-bADC}$$

The infarct volume was measured according the following formula: $\text{Vol} = XYZ \times 0.5 \text{ (cm}^3\text{)}$, where X , Y , and Z stand for the largest extension in x -, y -, and z -axis²³.

Circular regions of interest (ROI) on SPECT and MRI parametric maps, measuring 30 mm in diameter, were placed in the cerebellar hemispheres ipsilesional (I) and contralateral (C) to the hemispheric stroke. All ROIs were carefully placed to avoid the major vessels and the cerebellar vermis. To evaluate the inter-reader reproducibility, these ROIs were drawn by two experienced neuroradiologists both with 5 years of experience. A $\text{CBF}_{\text{SPECT}}$ asymmetry index (AI_{SPECT}) was calculated by using the following equation:

$$\text{AI}_{\text{SPECT}} = (\text{CBF}_I - \text{CBF}_C) / (\text{CBF}_I + \text{CBF}_C) \times 100\%$$

The presence of CCD was defined as $\text{AI}_{\text{SPECT}} \geq 10\%$ ²⁴. AIs were also calculated for mean f , D^* , and CBF_{ASL} in all subjects according to:

$$\text{AI}_f = (f_I - f_C) / (f_I + f_C) \times 100\%$$

$$\text{AI}_{D^*} = (D^*_I - D^*_C) / (D^*_I + D^*_C) \times 100\%$$

$$\text{AI}_{\text{ASL}} = (\text{CBF}_I - \text{CBF}_C) / (\text{CBF}_I + \text{CBF}_C) \times 100\%$$

Statistical analysis

All data were expressed as mean ± standard deviation (SD). Statistical analysis was performed using SPSS 20.0 (SPSS, Chicago, IL, USA). Patients were divided into CCD-positive and CCD-negative groups according to their AI_{SPECT} . Descriptive data from CCD-positive and CCD-negative groups were analyzed using either the Mann-Whitney U test or the Fisher exact test as appropriate. Paired t test was applied to compare IVIM-derived parameters (ADC , D , D^* , and f) and SPECT-/ASL-derived parameters (CBF) between the ipsilesional cerebellum and the contralateral cerebellum, respectively. To explore the relationships among $\text{CBF}_{\text{SPECT}}$, CBF_{ASL} , IVIM parameters, and clinical data, Pearson's correlation analysis was applied. Diagnostic performance (sensitivity, specificity, positive likelihood ratio (+LR), and negative likelihood ratio (-LR)) of IVIM parameters in CCD diagnosis was done by using receiver

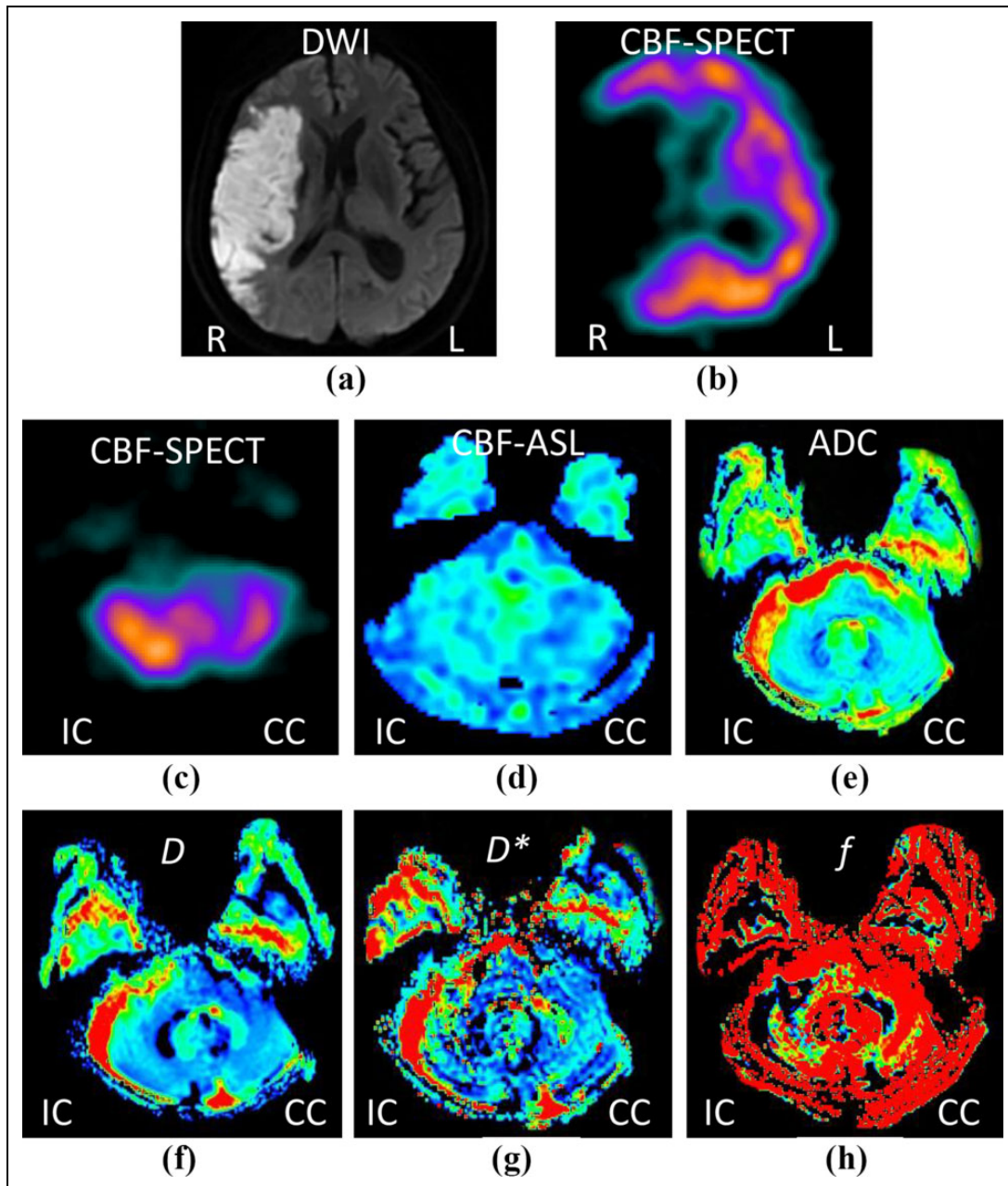


Figure 1. A 65-year-old man with supratentorial stroke in the right parietal for 10 days: hyperintensity stroke lesion can be recognized on the diffusion weighted image (DWI) ($b = 1000 \text{ sec/mm}^2$) (a). SPECT maps show hypoperfusion in the same lesion (b). SPECT maps (c) and ASL imaging (d) show hypoperfusion in the contralateral cerebellum. The IVIM-derived ADC (e) and D (f) maps have no change between the ipsilesional cerebellum and the contralateral cerebellum, whereas D^* (g) and f (h) values show a difference in the ipsilesional cerebellum compared with those in the contralateral hemisphere. CCD: crossed cerebellar diaschisis; CBF: cerebral blood flow; SPECT: single-photon emission computed tomography; ASL: arterial spin-labeling MR imaging; IC: ipsilateral cerebellum; CC: contralateral cerebellum; ADC: the apparent diffusion coefficient; D: slow diffusion coefficient; D^* : fast diffusion coefficient; f : vascular volume fraction.

operating characteristics (ROC) curve analysis. Statistical significance was defined as $p < 0.05$, $p < 0.01$ (two tailed).

Results

Among all 39 eligible patients enrolled in this study, 13 (33.3%) exhibited CCD based on their SPECT results, the

standard reference. As shown in Table 1, no significant difference in age or sex distribution was observed between CCD-positive and CCD-negative groups (both $p > 0.01$). However, the admission NIHSS score and infarct volume in the CCD-positive group were significantly higher than those in the CCD-negative group ($p = 0.02$ and $p = 0.042$, respectively). The NIHSS score was significantly lower at

Table 2. Comparison of different parameters in bilateral cerebellum.

Parameters	IC	CC	p value
CCD+			
CBF _{SPECT} (ml/100g/min)	85.93 ± 25.84	72.85 ± 21.48	<0.0001*
CBF _{ASL} (ml/100g/min)	40.92 ± 9.08	33.96 ± 9.04	<0.0001*
ADC (× 10 ⁻³ mm ² /s)	0.74 ± 0.07	0.76 ± 0.07	0.30
D (× 10 ⁻³ mm ² /s)	0.61 ± 0.05	0.61 ± 0.04	0.53
D* (× 10 ⁻³ mm ² /s)	9.06 ± 2.25	6.84 ± 1.86	0.0001*
f (× 10 ⁻³ mm ² /s)	0.20 ± 0.07	0.25 ± 0.09	0.001*
CCD-			
CBF _{SPECT} (ml/100g/min)	77.94 ± 28.50	76.02 ± 27.09	0.009*
CBF _{ASL} (ml/100g/min)	42.37 ± 9.58	42.37 ± 9.58	0.134
ADC (× 10 ⁻³ mm ² /s)	0.73 ± 0.08	0.75 ± 0.09	0.186
D (× 10 ⁻³ mm ² /s)	0.60 ± 0.04	0.60 ± 0.05	0.28
D* (× 10 ⁻³ mm ² /s)	8.28 ± 2.2	8.55 ± 2.4	0.409
f (× 10 ⁻³ mm ² /s)	0.23 ± 0.08	0.22 ± 0.08	0.383

CCD: crossed cerebellar diaschisis; CBF: cerebral blood flow; SPECT: single-photon emission computed tomography; ASL: arterial spin-labeling magnetic resonance imaging; IC: ipsilateral cerebellum; CC: contralateral cerebellum; ADC: the apparent diffusion coefficient; D: slow diffusion coefficient; D*: fast diffusion coefficient; f, vascular volume fraction.

Values are mean ± standard deviation. *Results indicate a significant difference ($p < 0.01$).

discharge than at admission in the CCD-negative group ($p = 0.021$), whereas no significant difference was found between the admission and discharge NIHSS scores in the CCD-positive group ($p = 0.724$). In the CCD-positive group ($n = 13$), infarcts were located in the gray matter in eight (61.5%), the white matter in five (38.5%), and the thalamus in zero (0%) patients. We also found that patients with lesions in the gray matter were more likely to suffer CCD ($p = 0.005$) (Table 1).

Figure 1 shows the images of diffusion weighted image (DWI) ($b = 1000 \text{ sec/mm}^2$) (a), SPECT (b, c), ASL (d), and maps of IVIM parameters ADC (e), D (f), D* (g), f (h) of representative patients with supratentorial stroke in the left parietal lobe for 10 days. Paired t tests were used to compare the average values of these parameters between ipsilesional and contralateral cerebellums in CCD-positive and CCD-negative groups, respectively. As shown in Tables 2 and 3, D*, CBF_{ASL}, and CBF_{SPECT} of the contralateral cerebellum were significantly lower than those of the ipsilesional cerebellum in the CCD-positive group ($p = 0.0001$, $p < 0.0001$ and $p < 0.0001$, respectively), whereas f was significantly higher ($p = 0.001$), and no statistical difference was observed in D and ADC ($p = 0.53$ and $p = 0.30$, respectively). In the CCD-negative group, all IVIM parameters did not significantly differ between the contralateral and the ipsilesional cerebellums ($p > 0.05$).

The results of Pearson's correlation analysis are presented in Table 4. Although no significant correlation was detected between D* and CBF_{SPECT} or between D* and CBF_{ASL}, there were positive correlations between AI_D* and AI_{SPECT}, as well

Table 3. D* and AI_D* parameters in stroke patients.

Patients	IC (× 10 ⁻³ mm ² /s)	CC (× 10 ⁻³ mm ² /s)	AI _D * (%)
CCD+			
1	10.7	6.16	27
2	9.2	6.9	14
3	12	11.5	2
4	8.75	7.28	9
5	5.63	4.68	9
6	9.54	7.28	13
7	12.5	7.78	23
8	9.01	6.03	20
9	8.07	6.02	15
10	6.55	6.29	20
11	5.34	4.33	10
12	7.32	5.81	12
13	13.2	8.9	20
CCD-			
1	11.2	11.6	-1.7
2	7.24	11.2	-21
3	6.73	5.46	10.4
4	12.4	10.6	7.8
5	6.35	9.58	-20
6	6.27	5.35	8.0
7	10.7	10.4	-20
8	6.79	6.76	8.0
9	12.6	11.6	1.4
10	5.35	6.56	0.2
11	6.27	5.76	4.1
12	9.48	7.77	-10
13	6.44	5.84	4.2
14	6	9.5	10
15	9.26	8.79	4.9
16	11.1	10.3	2.2
17	8.48	7.39	2.6
18	10.7	10.4	3.7
19	6.92	7.39	6.9
20	11	10.9	1.4
21	8.15	8.21	-0.03
22	8.02	8.01	0
23	5.53	9.11	-24.4
24	8.16	7.12	6.8
25	6.26	6.35	-0.7
26	7.89	10.6	-14

CCD: crossed cerebellar diaschisis; IC: ipsilateral cerebellum; CC: contralateral cerebellum; D*: fast diffusion coefficient; AI: asymmetry index.

as between AI_D* and AI_{ASL} ($r = 0.48$, $p = 0.002$; $r = 0.502$, $p = 0.001$, respectively) (Figure 2). The AI_f value had a negative correlation with both AI_{SPECT} and AI_{ASL} ($r = -0.325$, $p = 0.04$; $r = -0.347$, $p = 0.03$, respectively). The area under the ROC curve value of AI_D* for CCD diagnosis was 0.923 (Figure 3). The sensitivity, specificity, +LR, and -LR values of AI_D* in CCD diagnosis were 84.6%, 92.3%, 10.9, and 0.16 respectively, at the optimal cut-off value of 8.54%.

Discussion

In the present study, we evaluated whether IVIM could predict CCD in patients with supratentorial stroke. We found

Table 4. The results of Pearson's correlation between various parameters.

Parameters	<i>r</i> value	<i>p</i> value
D* and CBF _{SPECT}	0.079	0.492
D* and CBF _{ASL}	0.203	0.072
<i>f</i> and CBF _{SPECT}	-0.104	0.195
<i>f</i> and CBF _{ASL}	-0.046	0.687
AI _{D*} and AI _{SPECT}	0.48	0.002*
AI _{D*} and AI _{ASL}	0.502	0.001*
AI _{<i>f</i>} and AI _{SPECT}	-0.325	0.04*
AI _{<i>f</i>} and AI _{SPECT}	-0.347	0.03*

AI: asymmetry index. CBF: cerebral blood flow; SPECT: single-photon emission computed tomography; ASL: arterial spin-labeling magnetic resonance imaging; D*, fast diffusion coefficient; *f*, vascular volume fraction. Values are mean ± standard deviation. *Results indicate a significant difference (*p* < 0.05).

that D* was decreased in the contralateral cerebellum compared with in the ipsilesional cerebellum in CCD-positive cases. Furthermore, we determined the optimal cutoff value for AI_{D*} and analyzed its reliability in CCD detection.

According to recent literature on CCD, decreased blood flow and metabolism were more commonly observed in the contralateral cerebellum compared with the ipsilesional side using PET and SPECT methods^{9,25}. Although these imaging methods have enhanced our understanding of CCD, the requirement of radioactive tracers and lack of spatial resolution limit their application in the clinical setting. With the development of MR perfusion techniques, several studies have been carried out to detect CCD by noninvasive MRI. ASL takes endogenous arterial water as a diffusible tracer, which enables us to estimate brain perfusion frequently over a long-term follow-up period⁴. A previous study indicated

that ASL could identify CCD by using asymmetric CBF_{ASL}²⁶.

As a new contrast-free imaging method, IVIM could separate microcirculation or perfusion effects from true diffusion by applying DWI obtained with multiple *b* values and a bi-exponential model. It has been proven that IVIM can monitor the change in cerebral blood flow in a gradual way after the vasodilation or vasoconstriction induced by CO₂ and O₂¹⁷. In stroke cases, IVIM analysis showed a significant reduction in D, D*, and *f* values in lesions compared with the contralateral side²⁰. In our previous study, we successfully assessed the tissue diffusion and perfusion parameters simultaneously in ischemic stroke patients by using IVIM-MRI²⁷. The studies mentioned above implied it was feasible to measure the perfusion of brain tissue by IVIM.

In our present study, IVIM imaging was applied to detect CCD, which has rarely been reported in previous studies. In CCD-positive cases, patients had lower D* and higher *f* values in contralateral cerebellum compared with those in the ipsilesional cerebellum, but no significant difference was observed in ADC or D, which implied the CCD was related to changes of the microvascular perfusion but not tissue microstructure indicated by diffusivity. This finding is consistent with the results reported by Meyer et al., revealing that CCD was directly related to the loss of afferent stimuli from the supratentorial cortex, but not structural change in animal models²⁸. Similarly, in another previous study, a reduction in perfusion-related CBF value was observed in the contralateral cerebellum of CCD-positive stroke patients using contrast-based imaging modalities¹². Although D* did not have a direct correlation with CBF_{SPECT} and CBF_{ASL}, AI_{D*} was found to have a positive correlation with AI_{SPECT} and AI_{ASL} in our study. A significant positive correlation was also observed between D* and CBF_{ASL} in both tumor and

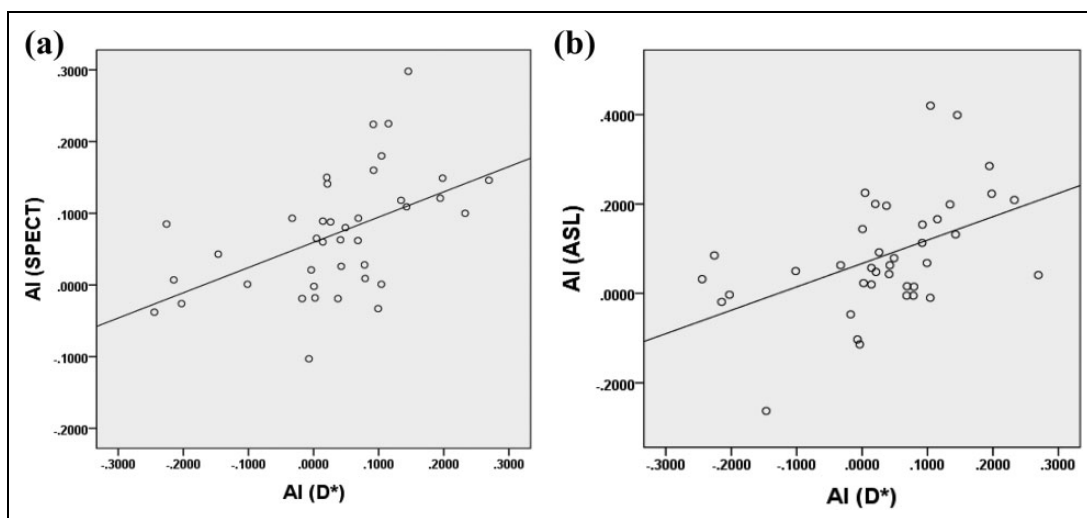


Figure 2. The scatter plot for the relationships between AI_{D*} and AI_{SPECT} (a) (*r* = 0.48, *p* = 0.002) and between AI_{D*} and AI_{ASL} (b) (*r* = 0.502, *p* = 0.001). AI: asymmetry index; SPECT: single-photon emission computed tomography; ASL: arterial spin-labeling magnetic resonance imaging; D*: fast diffusion coefficient.

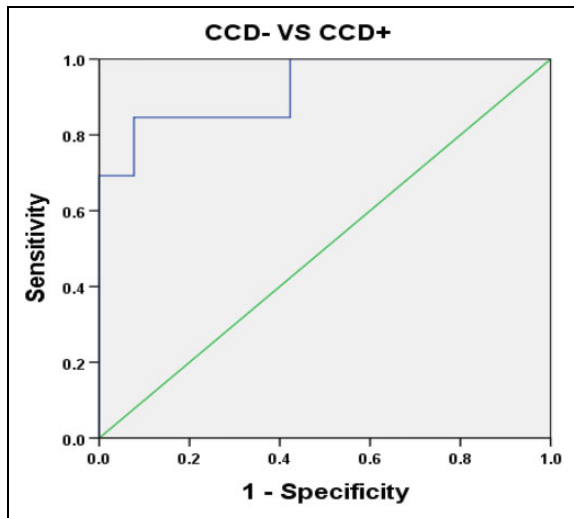


Figure 3. Receiver operating characteristic (ROC) curves for AI_{D^*} in patients based on AI_{SPECT} . AI: asymmetry index; SPECT: single-photon emission computed tomography; D^* = fast diffusion coefficient.

white matter by Lin et al¹⁸. Therefore, D^* derived from the IVIM model can reflect cerebral perfusion and may be an alternative parameter in the assessment of CCD in stroke.

Theoretically, the volume fraction of the rapid diffusion component, the f value, is expected to be lower in the contralateral cerebellum of CCD. Interestingly, we observed a higher f value in the contralateral cerebellum of the CCD-positive group, which is inconsistent with the reported hypoperfusion, such as reduced perfusion in the contralateral cerebellum of patients with CCD^{10,29}, using other imaging techniques. According to previous studies, two facts might explain this phenomenon: different choices of b values and times of echo (TE). A lower b value contributes to the pseudodiffusion component³⁰. Thus, the b values might be important for calculating the f value accurately. Lemke et al. demonstrated that f was influenced by TE; the longer the TE, the greater the signal attenuation at low b values and the higher the f value³¹. On top of that, cautious interpretation of f in supratentorial stroke with CCD is needed, as f itself might not purely reflect capillary blood flow within each voxel³². Moreover, we also found the AI_f value has a negative correlation with AI_{SPECT} and AI_{ASL} , respectively. Therefore, further studies are needed to investigate this in more detail. IVIM can provide both diffusion and perfusion imaging information, which has the advantage of providing more opportunities to further explore the clinical value of IVIM in the brain. Furthermore, as a radiation and contrast-free method, IVIM could be more beneficial to patients than other imaging methods.

The incidence of CCD in our clinical subjects was 33.3% using SPECT, whereas various values were reported by other studies using different imaging methods: 15.61% using dynamic susceptibility contrast MRI¹², 31% using CT

perfusion³³, 39.8% using SPECT²⁴, 52% using ASL MRI¹⁴, and 89% using PET³⁴. Such differences could be attributed to multiple factors, such as the median time interval from onset to image acquisition, the differences in patient selection criteria, and the imaging principles. In our study, the infarct volume was significantly larger and the admission NIHSS score was significantly higher in the CCD-positive than in the CCD-negative group. Meanwhile, the NIHSS score decreased significantly in the CCD-negative group at discharge, but there was no significant difference between admission and discharge NIHSS scores in the CCD-positive group. These results demonstrated the NIHSS score and infarct volume were closely related to being CCD positive, and that patients with CCD may have a worse outcome than those without CCD in subacute stroke. Previously, a PET study on CCD detecting reported the volume of supratentorial infarct volume played a significant role in CCD development³⁵. Shinohara et al. proved that the asymmetry index of the contralateral cerebellar hemisphere was significantly correlated with NIHSS score using 3D ASL²⁹.

As for the location of lesions in our study, CCD was found to be more frequent in patients with infarcts in the gray matter. Meanwhile, Forster et al. indicated that CCD was a frequent phenomenon in acute thalamic infarct³⁶. However, some other studies suggested that lesions in other locations such as the frontal lobe and the temporal lobe could contribute to the occurrence of CCD^{37,38}. The discrepancies may be explained by factors such as the number of cases or classification method and so on.

Conclusion

In this study, for the first time we demonstrated that CCD could be diagnosed with IVIM by a decreased D^* value in the contralateral cerebellum compared with that in the ipsilesional side. Furthermore, we report that AI_{D^*} has a statistically significant correlation with AI_{ASL} and AI_{SPECT} , respectively. Consequently, as a noninvasive quantitative MRI method, IVIM could obtain perfusion characteristics and might be a novel method of assessing supratentorial stroke with CCD. Based on the findings above, IVIM could be a novel valuable imaging technique in detecting CCD with the advantage in predicting outcome of patients with CCD.

Declaration of Conflicting Interests

The author(s) declared no potential conflicts of interest with respect to the research, authorship, and/or publication of this article.

Ethical Approval

This study was approved from the hospital institutional research ethics board.

Funding

The author(s) disclosed receipt of the following financial support for the research, authorship, and/or publication of this article: this

work was supported by the Foundation of Renji Hospital South Campus, Shanghai Jiao Tong University School of Medicine. (Nos 2017PYQB04, 2016PWGY02); Shanghai Municipal Natural Science Foundation (16ZR1420700); Medical Guidance Project from Shanghai Science and Technology Committee (19411971200).

ORCID iD

Juan Wang  <https://orcid.org/0000-0001-8978-462X>

Statement of Human and Animal Rights

The whole study followed approval from the hospital institutional research ethics board, and all subjects have written informed consent.

Statement of Informed Consent

All subjects have written informed consent.

References

1. Wu KJ, Yu S, Lee JY, Hoffer B, Wang Y. Improving neuror-epair in stroke brain through endogenous neurogenesis-enhancing drugs. *Cell Transplant*. 2017;26(9):1596–1600.
2. Strother MK, Buckingham C, Faraco CC, Arteaga DF, Lu P, Xu Y, Donahue MJ. Crossed cerebellar diaschisis after stroke identified noninvasively with cerebral blood flow-weighted arterial spin labeling MRI. *Eur J Radiol*. 2016;85(1):136–142.
3. Calabria F, Schillaci O. Recurrent glioma and crossed cerebellar diaschisis in a patient examined with 18F-DOPA and 18F-FDG PET/CT. *Clin Nucl Med*. 2012;37(9):878–879.
4. Kang KM, Sohn CH, Choi SH, Jung KH, Yoo RE, Yun TJ, Kim JH, Park SW. Detection of crossed cerebellar diaschisis in hyperacute ischemic stroke using arterial spin-labeled MR imaging. *PLoS One*. 2017;12(3):e0173971.
5. Kellner-Weldon F, El-Koussy M, Jung S, Jossen M, Klinger-Gratz PP, Wiest R. Cerebellar hypoperfusion in migraine attack: Incidence and significance. *AJNR Am J Neuroradiol*. 2018; doi:10.3174/ajnr.A5508. PMID: 29326138.
6. Ferilli MAN, Brunetti V, Costantini EM, Della Marca G. Left hemispheric status epilepticus with crossed cerebellar diaschisis. *J Neurol Neurosurg Psychiatry*. 2018;89(3):311–312.
7. Agarwal KK, Tripathi M, Karunanithi S, Das CJ, Suri V, Nalwa A. Crossed cerebellar diaschisis in cerebral toxoplasmosis demonstrated on (1)(8)F-FDG PET/CT. *Rev Esp Med Nucl Imagen Mol*. 2014;33(6):397–398.
8. Szilagyi G, Vas A, Kerenyi L, Nagy Z, Csiba L, Gulyas B. Correlation between crossed cerebellar diaschisis and clinical neurological scales. *Acta Neurol Scand*. 2012;125(6):373–381.
9. Takasawa M, Watanabe M, Yamamoto S, Hoshi T, Sasaki T, Hashikawa K, Matsumoto M, Kinoshita N. Prognostic value of subacute crossed cerebellar diaschisis: single-photon emission CT study in patients with middle cerebral artery territory infarct. *AJNR Am J Neuroradiol*. 2002;23(2):189–193.
10. Kunz WG, Sommer WH, Hohne C, Fabritius MP, Schuler F, Dorn F, Othman AE, Meinel FG, von Baumgarten L, Reiser MF, Ertl-Wagner B, et al. Crossed cerebellar diaschisis in acute ischemic stroke: Impact on morphologic and functional outcome. *J Cereb Blood Flow Metab*. 2017;37(11):3615–3624.
11. Baron JC, Bousser MG, Comar D, Castaigne P. “Crossed cerebellar diaschisis” in human supratentorial brain infarction. *Trans Am Neurol Assoc*. 1981;105:459–461.
12. Lin DD, Kleinman JT, Wityk RJ, Gottesman RF, Hillis AE, Lee AW, Barker PB. Crossed cerebellar diaschisis in acute stroke detected by dynamic susceptibility contrast MR perfusion imaging. *AJNR Am J Neuroradiol*. 2009;30(4):710–715.
13. Liu Y, Karonen JO, Nuutinen J, Vanninen E, Kuikka JT, Vanninen RL. Crossed cerebellar diaschisis in acute ischemic stroke: a study with serial SPECT and MRI. *J Cereb Blood Flow Metab*. 2007;27(10):1724–1732.
14. Chen S, Guan M, Lian HJ, Ma LJ, Shang JK, He S, Ma MM, Zhang ML, Li ZY, Wang MY, Shi DP, et al. Crossed cerebellar diaschisis detected by arterial spin-labeled perfusion magnetic resonance imaging in subacute ischemic stroke. *J Stroke Cerebrovasc Dis*. 2014;23(9):2378–2383.
15. Gao QQ, Lu SS, Xu XQ, Wu CJ, Liu XL, Liu S, Shi HB. Quantitative assessment of hyperacute cerebral infarction with intravoxel incoherent motion MR imaging: Initial experience in a canine stroke model. *J Magn Reson Imaging*. 2017;46(2):550–556.
16. Le Bihan D, Breton E, Lallemand D, Aubin ML, Vignaud J, Laval-Jeantet M. Separation of diffusion and perfusion in intravoxel incoherent motion MR imaging. *Radiology*. 1988;168(2):497–505.
17. Federau C, Maeder P, O’Brien K, Browaeys P, Meuli R, Hagmann P. Quantitative measurement of brain perfusion with intravoxel incoherent motion MR imaging. *Radiology*. 2012;265(3):874–881.
18. Lin Y, Li J, Zhang Z, Xu Q, Zhou Z, Zhang Z, Zhang Y, Zhang Z. Comparison of intravoxel incoherent motion diffusion-weighted MR imaging and arterial Spin labeling MR imaging in Gliomas. *Biomed Res Int*. 2015;2015:234245.
19. Li GF, Duan SJ, Yan LF, Wang W, Jing Y, Yan WQ, Sun Q, Wang SM, Nan HY, Xu TY, Zheng DD, et al. Intravoxel incoherent motion diffusion-weighted MR imaging parameters predict pathological classification in thymic epithelial tumors. *Oncotarget*. 2017. 2017;8(27):44579–44592.
20. Yao Y, Zhang S, Tang X, Zhang S, Shi J, Zhu W, Zhu W. Intravoxel incoherent motion diffusion-weighted imaging in stroke patients: initial clinical experience. *Clin Radiol*. 2016;71(9):938 e11–938 e16.
21. Federau C, Sumer S, Becce F, Maeder P, O’Brien K, Meuli R, Wintermark M. Intravoxel incoherent motion perfusion imaging in acute stroke: initial clinical experience. *Neuroradiology*. 2014;56(8):629–635.
22. Kim HS, Kim DI, Lee JD, Jeong EK, Chung TS, Yoon PH, Lee SK, Kim EJ, Yoon YK, Suh BC, Lee BI. Significance of 99mTc-ECD SPECT in acute and subacute ischemic stroke: comparison with MR images including diffusion and perfusion weighted images. *Yonsei Med J*. 2002;43(2):211–222.
23. van der Worp HB, Claus SP, Bar PR, Ramos LM, Algra A, van Gijn J, Kappelle LJ. Reproducibility of measurements of cerebral infarct volume on CT scans. *Stroke*. 2001;32(2):424–430.
24. Komaba Y, Mishina M, Utsumi K, Katayama Y, Kobayashi S, Mori O. Crossed cerebellar diaschisis in patients with cortical

- infarction: logistic regression analysis to control for confounding effects. *Stroke*. 2004;35(2):472–476.
25. Takuwa H, Tajima Y, Kokuryo D, Matsuura T, Kawaguchi H, Masamoto K, Taniguchi J, Ikoma Y, Seki C, Aoki I, Tomita Y, et al. Hemodynamic changes during neural deactivation in awake mice: a measurement by laser-Doppler flowmetry in crossed cerebellar diaschisis. *Brain Res*. 2013;1537:350–355.
 26. O’Gorman RL, Siddiqui A, Alsop DC, Jarosz JM. Perfusion MRI demonstrates crossed-cerebellar diaschisis in sickle cell disease. *Pediatr Neurol*. 2010;42(6):437–440.
 27. Suo S, Cao M, Zhu W, Li L, Li J, Shen F, Zu J, Zhou Z, Zhuang Z, Qu J, Chen Z, et al. Stroke assessment with intravoxel incoherent motion diffusion-weighted MRI. *NMR Biomed*. 2016; 29(3):320–328.
 28. Meyer JS, Obara K, Muramatsu K. Diaschisis. *Neurol Res*. 1993;15(6):362–366.
 29. Shinohara Y, Kato A, Kuya K, Okuda K, Sakamoto M, Kowa H, Ogawa T. Perfusion MR imaging using a 3D pulsed continuous arterial spin-labeling method for acute cerebral infarction classified as branch atheromatous disease involving the lenticulostriate artery territory. *AJNR Am J Neuroradiol*. 2017;38(8):1550–1554.
 30. Cohen AD, Schieke MC, Hohenwarter MD, Schmainda KM. The effect of low b-values on the intravoxel incoherent motion derived pseudodiffusion parameter in liver. *Magn Reson Med*. 2015;73(1):306–311.
 31. Lemke A, Laun FB, Simon D, Stieltjes B, Schad LR. An in vivo verification of the intravoxel incoherent motion effect in diffusion-weighted imaging of the abdomen. *Magn Reson Med*. 2010;64(6):1580–1585.
 32. Wong SM, Zhang CE, van Bussel FC, Staals J, Jeukens CR, Hofman PA, van Oostenbrugge RJ, Backes WH, Jansen JF. Simultaneous investigation of microvasculature and parenchyma in cerebral small vessel disease using intravoxel incoherent motion imaging. *Neuroimage Clin*. 2017;14:216–221.
 33. Jeon YW, Kim SH, Lee JY, Whang K, Kim MS, Kim YJ, Lee MS, Brain Research G. Dynamic CT perfusion imaging for the detection of crossed cerebellar diaschisis in acute ischemic stroke. *Korean J Radiol*. 2012;13(1):12–19.
 34. Miura H, Nagata K, Hirata Y, Satoh Y, Watahiki Y, Hatazawa J. Evolution of crossed cerebellar diaschisis in middle cerebral artery infarction. *J Neuroimaging*. 1994;4(2):91–96.
 35. Sobesky J, Thiel A, Ghaemi M, Hilker RH, Rudolf J, Jacobs AH, Herholz K, Heiss WD. Crossed cerebellar diaschisis in acute human stroke: a PET study of serial changes and response to supratentorial reperfusion. *J Cereb Blood Flow Metab*. 2005;25(12):1685–1691.
 36. Forster A, Kerl HU, Goerlitz J, Wenz H, Groden C. Crossed cerebellar diaschisis in acute isolated thalamic infarction detected by dynamic susceptibility contrast perfusion MRI. *PLoS One*. 2014;9(2):e88044.
 37. Kamouchi M, Fujishima M, Saku Y, Ibayashi S, Iida M. Crossed cerebellar hypoperfusion in hyperacute ischemic stroke. *J Neurol Sci*. 2004;225(1-2):65–69.
 38. Liu ZC, Yan LF, Hu YC, Sun YZ, Tian Q, Nan HY, Yu Y, Sun Q, Wang W, Cui GB. Combination of IVIM-DWI and 3D-ASL for differentiating true progression from pseudoprogression of Glioblastoma multiforme after concurrent chemoradiotherapy: study protocol of a prospective diagnostic trial. *BMC Med Imaging*. 2017;17(1):10.